hydrology

MDPI

Article

Evaluation of Gridded Rainfall Products in Three West African Basins

Omar Goudiaby [1], Ansoumana Bodian [1,*], Alain Dezetter [2], Ibrahima Diouf [3] and Andrew Ogilvie [4]

[1] Laboratoire Leïdi—Dynamique des Territoires et Développement, Université Gaston Berger (UGB), Saint-Louis BP 234, Senegal; goudiaby.omar@ugb.edu.sn
[2] HydroSciences Montpellier, University of Montpellier, IRD, CNRS, UFR Pharmacie, Bâtiment HYDROPOLIS, 15 Avenue Charles Flahaut, 34090 Montpellier, France; alain.dezetter@ird.fr
[3] Laboratoire de Physique de l'Atmosphère et de l'Océan-Simon Fongang, Ecole Supérieure Polytechnique de l'Université Cheikh Anta Diop (UCAD), BP 5085 Dakar-Fan, Dakar 10700, Senegal; ibrahima23.diouf@ucad.edu.sn
[4] UMR G-EAU, AgroParisTech, BRGM, CIRAD, INRAE, Institut Agro, IRD, University of Montpellier, 34196 Montpellier, France; andrew.ogilvie@ird.fr
* Correspondence: ansoumana.bodian@ugb.edu.sn; Tel.: +221-77-811-7553

Abstract: In recent years, accessing rainfall data from ground observation networks maintained by national meteorological services in West Africa has become increasingly challenging. This is primarily due to high acquisition costs and the often sparse distribution of rainfall gauges across the region, which limits their use in hydrological studies and related research. At the same time, the rising availability of precipitation products derived from satellite/earth observations, reanalysis datasets, and in situ measurements presents exciting prospects for hydrological applications. Nonetheless, these datasets constitute indirect measurements, necessitating rigorous validation against ground-based rainfall data. This study comprehensively assesses twenty-three gridded rainfall products, including sixteen from satellites, six from reanalysis data, and one from in situ measurements, across the Senegal, Gambia, and Casamance River basins. Performance evaluation is conducted across distinct climatic zones, both pre- and post-resampling against observed rainfall data gathered from forty-nine rainfall stations over a six-year period (2003–2008). Evaluation criteria include the Kling–Gupta Efficiency (KGE) and Percentage of Bias (PBIAS) metrics, assessed at daily, monthly, and seasonal time steps. The results reveal distinct performance levels among the evaluated rainfall products. RFE, ARC2, and CPC notably yield the highest KGE scores at the daily time step, while GPCP, CHIRP, CHIRPS, RFE, MSWEP, ARC2, CPC, TAMSAT, and CMORPHCRT demonstrate superior performance at the monthly time step. During the rainy season, these products generally exhibit robustness. However, rainfall estimates derived from reanalysis datasets (ERA5, EWEMBI, MERRA2, PGF, WFDEICRU, and WFDEIGPCC) perform poorly in the studied basins. Based on the PBIAS metric, most products tend to underestimate precipitation values, while only PERSIANN and PERSIANNCCS lead to significant overestimations. Spatially, optimal performance of the products is observed in the Casamance basin and the Sudanian and Sahelian climatic zones within the Gambia and Senegal basins. Conversely, in the Guinean zone of the Gambia and Senegal Rivers, the rainfall products displayed the poorest performance.

Keywords: gridded precipitation products; Casamance River; Gambia River; Senegal River; West Africa

Citation: Goudiaby, O.; Bodian, A.; Dezetter, A.; Diouf, I.; Ogilvie, A. Evaluation of Gridded Rainfall Products in Three West African Basins. *Hydrology* **2024**, *11*, 75. https://doi.org/10.3390/hydrology11060075

Academic Editor: Andrea Petroselli

Received: 22 April 2024
Revised: 21 May 2024
Accepted: 24 May 2024
Published: 29 May 2024

1. Introduction

The United Nations' World Population Prospects Report [1] highlights a steady population growth trend in West Africa. Projections indicate a population increase from 391 million in 2019 to 796 million by 2050, reaching approximately 1.5 billion by the end of the century. This demographic increase is expected to lead to a significant rise in water demand across various sectors, including domestic supply, industry, and intensified agriculture [2,3].

Against the backdrop of growing water demands, the drought experienced during the 1970s in West Africa drastically reduced water availability, with far-reaching impacts on socio-economic sectors [4–18]. In situations where water resources are limited and diverse users contend for access, competitive and conflicting scenarios may arise [19].

Given the prevailing challenges related to water resources, demographic growth, and potential climate change impacts, it becomes imperative to enhance our understanding of current and future water availability. This understanding is vital for effective water resource management and the implementation of adaptation strategies [20–22]. Knowledge of water resources is the cornerstone of optimal resource management [23] and depends on the availability of high-quality hydroclimatological data, derived from a dense network of ground stations over extended periods. Unfortunately, hydrometric services in several countries in West Africa face difficulties in gauging rivers and providing flow time series, due to human, material, and financial resource constraints [24,25]. Time series of observed data often suffer from incompleteness, discontinuity, and short durations, rendering them unsuitable for hydrological applications [26]. In parallel, access to in situ meteorological data, particularly at daily time steps, remains a major constraint due to the prohibitive costs of acquisition [27–29].

Meanwhile, the recent rise of precipitation products derived from satellites, reanalysis, and in situ data offers significant opportunities for hydrological applications, climate change studies, and sustainable water resource management [30–33]. Gridded precipitation data represent a valuable alternative to address issues related to the availability and accessibility of ground observations [34]. Gridded precipitation has a number of advantages: (i) near-global coverage, (ii) densification of measurement networks, (iii) fine spatiotemporal resolution, (iv) long-term availability, (v) accessibility, and so on. However, gridded rainfall estimates are indirect measurements characterized by spatial and temporal uncertainties that need to be evaluated and corrected where possible [35].

Several studies have directly compared gridded precipitation products with in situ data [35–37], while others have assessed their hydrological reliability at different time scales in West Africa [17,38–45].

For the direct comparison, Dembélé and Zwart [36] compared the reliability of seven products (ARC 2.0, CHIRPS, PERSIANN, RFE 2.0, TAMSAT, TARCAT, and TRMM) in Burkina Faso. Similarly, Satgé et al. [35] evaluated the performance of twenty-three mesh products (ARC-2, CHIRP v.2, CHIRPS v.2, CMORPH-Raw v.1, CMORPH-CRT v.1, CMORPH-BLD v.1, CPC v.1, GSMap-RT v.6, GSMap-Adj v.6, GPCC v.7, JRA-55 Adj, MSWEP v.2.2, PERSIANN-CDR, PERSIANN-RT, PERSIANN-Adj, SM2Rain-CCI b.2, TAMSAT v.3, TMPA-RT v.7, TMPA-Adj v.7, WFDEI, MERRA-2, JRA-55, and ERA-Interim) compared with in situ data from West Africa. The work of Didi et al. [37] focused on climate variability based on six rainfall indices in five countries (Senegal, Niger, Burkina Faso, Ivory Coast, and Benin) using CHIRPS data.

While for hydrological validation, Gosset et al. [39] assessed the ability of nine products (PERSIANN, CMORPH, TRMM, TMPA 3B42, GSMap, RFE, CPC, EPSAT, and GPCP-1DD) to simulate flows at AMMA-CATCH sites in Niger and Benin. Cassé et al. [40] analyzed the potential of six products (CPC, RFE2, TRMM 3B42 v7, TRMM 3B42RT, CMORPH, and PERSIANN) to predict flooding on the River Niger at Niamey. Gascon [17] used three products (TRMM, PERSIANN, and CMORPH) for a hydrological study of the Ouémé basin in Niger. In their paper, Poméon et al. [42] tested the effectiveness of ten products (CFSR, CHIRPS, CMORPH v1.0 CRT, CMORPH v1.0 Raw, PERSIANN-CDR, RFE 2.0, TAMSAT, TMPA 3B42 RT v7, and GPCC FDDv1) in West Africa. Bâ et al. [43] highlighted the importance of PERSIANN-CDR in hydrological modeling in the Senegal and Niger Rivers. Recently, Dembélé et al. [44] investigated the performance of seventeen gridded precipitation data (TAMSAT, CHIRPS, ARC, RFE, MSWEP, GSMap, PERSIANN-CDR, CMORPH-CRT, TRMM 3B42, TRMM 3B42RT, JRA-55, EWEMBI, WFDEI-GPCC, WFDEI-CRU, MERRA-2, PGF, and ERA5) in a simulation in the Volta basin of Burkina Faso. In a recent study, Kouakou et al. [45] used fifteen gridded precipitation products (ARC v.2,

CHIRP v.2, CHIRPS v.2, PERSIANN-CDR, MSWEP v2.2, TAMSAT v3, ERA5, JRA-55 Adj, MERRA-2 PRECTOT, MERRA-2 PRECTOTCORR, WFDEI-CRU, WFDEI-GPCC, CPC v.1, CRU TS v.4.00, and GPCC) to determine their reliability in simulating flows in different basins in West and Central Africa.

Compared with studies carried out exclusively on Senegal's main hydrosystems, Stisen and Sandholt [38] used five products (CMORPH, CCD, CPC-FEW v2, TRMM 3B46 v6, and PERSIANN) to simulate flows in Bafing Makana, Gourbassi, and Oualia, while Bodian et al. [41] simulated flows in Bafing Makana with TRMM.

However, most of these studies focus primarily on hydrological validation after spatial interpolation rather than direct/pixel-by-pixel evaluation against in situ rainfall data, and little is known of their performance across climatic zones. Additionally, some studies evaluated only a limited number of products, and the value of emerging datasets such as IMERG must be evaluated and compared across multiple regions and climates. Considering the importance of the Senegal, Gambia, and Casamance River basins in West Africa and the sparse research on the performance of gridded precipitation products in the region, this paper aims to evaluate the performance of twenty-three gridded rainfall products at daily, monthly, and seasonal time steps across these three river basins. Using a large number of products, this study also builds upon an exceptional database of ground-based rainfall observations from four countries and explores the performance of gridded datasets before and after spatial resampling across different time scales.

2. Materials and Methods

2.1. Study Area

This study focuses on the main hydrological systems of Senegal: the Casamance, Gambia, and Senegal River basins (refer to Figure 1). The Senegal River spans latitudes 10°30′ to 17°30′ north and longitudes 7°30′ to 16°30′ west, with a length of approximately 1,800 km [46]. Originating from the Bafing, Bakoye, and Falémé tributaries, sourced in the Fouta Djalon massif in Guinea, the basin covers an expansive area of 395.000 square kilometers [47]. This basin extends across the high plateau region of northern Guinea, the western part of Mali, the southern regions of Mauritania, and the northern part of Senegal [48]. The Gambia basin occupies the latitudinal range between 11°22′ and 14°40′ north and longitudinally between 11°13′ and 16°42′ west [49]. The Gambia River stretches across 1180 km [50] and drains an extensive area of 77.054 square kilometers, shared among Guinea, Senegal, and The Gambia [51]. The Casamance basin lies between 12°20′ and 13°21′ north latitude and 14°17′ and 16°47′ west longitude in the southern region of Senegal. Spanning approximately 300 km in length, the basin covers an area of 20.150 square kilometers [52]. While predominantly situated within Senegalese territory, it marginally extends into parts of the Republic of The Gambia to the north and Guinea-Bissau to the south [52–54].

The altitude varies significantly across these basins, ranging from 0 to 83 m for the Casamance basin, 0 to 1530 m for the Gambia basin, and for the Senegal basin (Figure 1a). Climatically, total rainfall plays a pivotal role in classification [40,46]. Over the period 1940–2004, the average annual rainfall (Figure 1b), according to Vintrou's [55] classification, indicates that the Casamance basin is situated within the Sudanian and Guinean climatic zones (extreme south), whereas the Gambia and Senegal basins encompass the Sahelian (extreme north), Sudanian, and Guinean (extreme south) climatic zones. Based on these climatic zones, the unimodal rainfall pattern is characterized by a wet season lasting three to six months and a dry season spanning nine to six months [16,47,50].

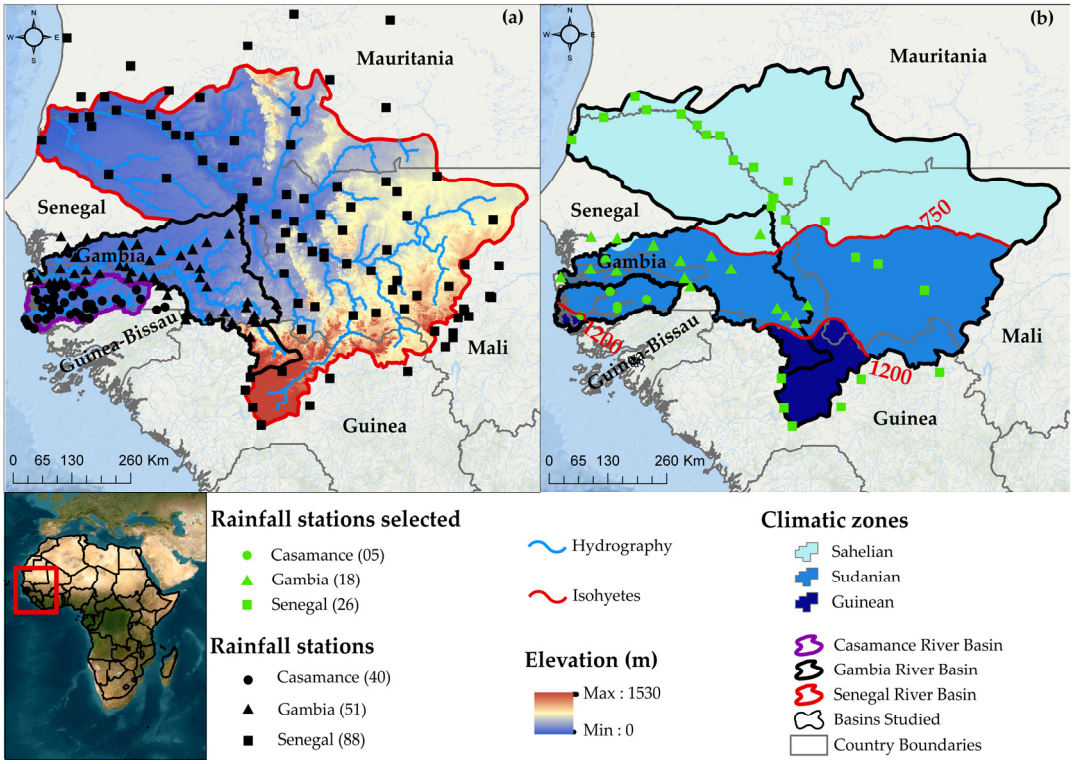

Figure 1. Location of the Casamance, Gambia, and Senegal River basins: (**a**) spatial distribution of altitudes and rainfall stations; (**b**) spatial distribution of selected rainfall stations and mean annual rainfall over the period 1940–2004.

2.2. Data

Two sources of data are used in this study: observed rainfall data and gridded rainfall products.

2.2.1. Observed Rainfall Data

The daily rainfall data utilized in this study originate from the national meteorological services of Senegal, Mali, Guinea, and The Gambia and are archived within the databases of the Senegal River Basin Organization (OMVS) and the Gambia River Basin Organization (OMVG). These datasets encompass observations from thirty-four stations within the Casamance basin, twenty-nine stations within the Gambia basin, and seventy-four stations within the Senegal basin. Figure 2 depicts the observed rainfall data collected across these three catchments. The temporal coverage of the datasets varies, spanning from 1950 to 2012 for the Casamance basin, 1950 to 2014 for the Gambia basin, and 1950 to 2019 for the Senegal basin.

Upon analysis of Figure 2, it becomes evident that the quality and continuity of these datasets differ among the basins. Among the one hundred and thirty-seven stations analyzed, only ten exhibit less than a 5% data gap, while most stations lack recent data. To ensure consistency and reliability in the analysis, a reference period spanning from 2003 to 2008 was selected for the statistical evaluation of the rainfall products (Figure 2). This timeframe offers the advantage of possessing complete and concurrent data across all forty-nine selected rainfall stations, comprising five stations for the Casamance basin, eighteen for the Gambia basin, and twenty-six for the Senegal basin (refer to Figure 1b). Furthermore, this period aligns with the recording timeframe of the majority of available gridded rainfall products (see Table 1).

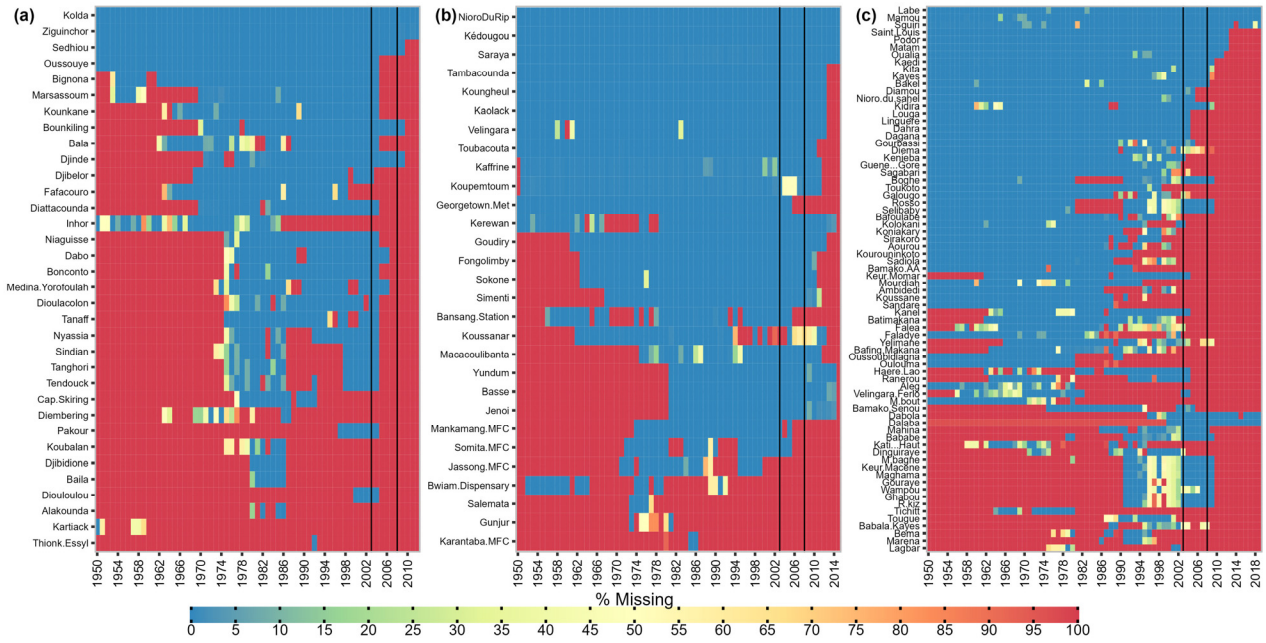

Figure 2. Inventory of daily rainfall data from stations selected for the three catchments: (**a**) Casamance, (**b**) Gambia, and (**c**) Senegal. The black lines on the graphs indicate the period used to evaluate the gridded rainfall products.

Table 1. Characteristics of the twenty-three gridded precipitation products selected.

Datasets	Full Product Name	Data Sources	Types	Start of Operation	Spatial Resolution	Temporal Resolution	References
ARC v2.0	Africa Rainfall Estimate Climatology v2.0	IS, S	Satellite	1983-P	0.1° × 0.1°	Daily	[56]
CHIRP v2.0	Climate Hazards Group InfraRed v2.0	S, R, A	Satellite	1981-P	0.05°	Daily	[57]
CHIRPS v2.0	Climate Hazard Group InfraRed Precipitation with Stations v2.0	IS, S, R, A	Satellite	1981-P	0.05°	Daily	[57]
MSWEP v2.2	Multi-Source Weighted-Ensemble Precipitation V2.2	IS, S, R, A	Satellite	1979-P	0.1° × 0.1°	3-hourly	[58–60]
TAMSAT v3.0	Tropical Applications of Meteorology using SATellite and ground-based observations v.3	IS, S	Satellite	1983-P	0.0375° × 0.0375°	Daily	[61,62]
GPCP-1DD v1.2	Global Precipitation Climatology Project 1-Degree Daily Combination v1.2	IS, S	Satellite	1997-P	1° × 1°	Daily	[63]
PERSIANN	Precipitation Estimation from Remotely Sensed Information using Artificial Neural Networks	S	Satellite	2000-P	0.25° × 0.25°	6h	[64,65]
PERSIANN-CDR v1r1	Precipitation Estimation from Remotely Sensed Information using Artificial Neural Networks Climate Data Record	IS, S	Satellite	1983-P	0.25° × 0.25°	Daily	[30]
PERSIANN-CCS	PERSIANN-Cloud Classification System	S	Satellite	2003-P	0.4° × 0.4°	Daily	[66]
PERSIANN-PDIR-NOW	PERSIANN-Dynamic Infrared Rain Rate near real-time		Satellite	2000-P	0.4° × 0.4°	Daily	[67]
PERSIANN-CCS-CDR	PERSIANN-Cloud Classification System- Climate Data Record	IS, S	Satellite	1983-P	0.4° × 0.4°	Daily	[68]
CMORPH-CRT v1.0	Climate Prediction Center MORPHing technique bias corrected v1.0	IS, S	Satellite	1998-2019	0.25° × 0.25°	Daily	[69,70]
RFE v2.0	Climate Prediction Center African Rainfall Estimate	IS, S	Satellite	2001-P	0.1° × 0.1°	Daily	[71,72]
IMERGDE v06	Integrated Multi-satellitE Retrievals for GPM (IMERG) Early	IS, S	Satellite	2000-P	0.1° × 0.1°	Daily	[73]
IMERGDL v06	Integrated Multi-satellitE Retrievals for GPM (IMERG) Late	IS, S	Satellite	2000-P	0.1° × 0.1°	Daily	[73]

Table 1. *Cont.*

Datasets	Full Product Name	Data Sources	Types	Start of Operation	Spatial Resolution	Temporal Resolution	References
IMERGDF v06	Integrated Multi-satellitE Retrievals for GPM (IMERG) Final	IS, S	Satellite	2000-P	0.1° × 0.1°	Daily	[73]
MERRA-2	Modern-Era Retrospective Analysis for Research and Applications 2	IS, S, R	Reanalysis	1980-P	0.5° × 0.5°	Hourly	[74,75]
ERA5	European Centre for Medium-range Weather Forecasts ReAnalysis 5 (ERA5)	R	Reanalysis	1979-P	0.25° × 0.25°	Hourly	[76]
EWEMBI v1.1	EartH2Observe, WFDEI, and ERA-Interim data Merged and Bias-corrected for ISIMIP (EWEMBI)	IS, R	Reanalysis	1979-2016	0.5° × 0.5°	Daily	[77]
PGF v3	Princeton University Global Meteorological Forcing	IS, R	Reanalysis	1979-2016	0.25° × 0.25°	Daily	[78]
WFDEI-CRU	WATCH Forcing Data ERAInterim (WFDEI) corrected using Climatic Research Unit (CRU)	IS, R	Reanalysis	1979-2018	0.5° × 0.5°	3-hourly/day	[79]
WFDEI-GPCC	WATCH Forcing Data ERAInterim (WFDEI) corrected using Global Precipitation Climatology Centre	IS, R	Reanalysis	1979-2016	0.5° × 0.5°	3-hourly/day	[80]
CPC v.1	Climate Prediction Center Unified v.1	IS	In situ	1979-P	0.5° × 0.5°	Daily	[81,82]

Read in the "Data Sources" column: IS, In situ; S, Satellite; R, Reanalysis; A, Analysis; and in the "Start of Operation" column, P, Present.

2.2.2. Gridded Precipitation Data

Multiple research entities and institutions have developed various gridded precipitation data products [82–84]. To streamline the selection process, three criteria were established: (i) thorough identification of available products through a literature review, (ii) ease of accessibility, and (iii) alignment of the product's registration period with the designated evaluation period (2003–2008) based on observed rainfall data inventory (refer to Figure 2). Ultimately, twenty-three products were chosen, encompassing sixteen satellite-based products (ARC v2.0, CHIRP, CHIRPS, CMORPH-CRT v1.0, GPCP-1DD v1.2, IMERGDE v06, IMERGDF v06, IMERGDL v06, MSWEP v2.2, PERSIANN, PERSIANN-CCS, PERSIANN-CDR v1r1, PERSIANN-CCS-CDR, PERSIANN-PDIR-NOW, RFE v2.0, and TAMSAT v3.0), six reanalysis products (ERA5, EWEMBI, PGF v3, MERRA2, WFDEI-CRU, and WFDEI-GPCC), and one in situ product (CPC v1.0/RT).

By evaluating a diverse range of products, this study aims to provide comprehensive insights into their performance across Senegal's main hydrological systems. The coordinates of the forty-nine selected stations (refer to Figure 1b) serve as reference points for extracting gridded rainfall data. Table 1 provides a summary of the characteristics of each product, along with corresponding references for further details on their development and methodologies.

2.3. Methods

Considering the variations in spatial and temporal resolutions among the products (as outlined in Table 1), the initial step involved temporal and spatial resampling. Subsequently, a comprehensive point-by-pixel assessment was conducted utilizing two statistical criteria: Kling–Gupta Efficiency (KGE) and Percentage Bias (PBIAS).

2.3.1. Temporal Resampling of Products

The gridded precipitation products under assessment exhibit diverse temporal resolutions (refer to Table 1). To facilitate a comprehensive evaluation, this study assesses these products at daily, monthly, and seasonal intervals. Consequently, temporal aggregation is performed to align the products with these specific time steps, including daily, monthly, and seasonal aggregations.

For seasonal assessments, only the rainy season is considered, with its duration varying across climatic zones. Drawing from previous studies focused on characterizing the rainy season in West Africa [28,50,85], specific periods have been selected for this study. These periods are delineated as follows: three months for the Sahelian zone (July to September), five months for the Sudanian zone (June to October), and six months for the Guinean zone (May to October).

2.3.2. Spatial Resampling of Products

Spatial resampling serves to establish a uniform resolution for all selected gridded precipitation data, allowing for a comparative assessment against the initial datasets. Given the differing spatial resolutions among the data products (as detailed in Table 1), it is imperative to initially evaluate them at their native resolutions. This ensures a precise comparison between observed rainfall data and the corresponding pixel values at the same station.

Subsequently, an appropriate grid is defined for all products to standardize the spatial resolution. To assess the impact of this new grid on data performance, grids for each spatial resolution are extracted and overlaid onto the selected stations. Appendix A illustrates this overlay, depicting the alignment between rainfall stations and different grids. The objective is to identify the resolution that accommodates the fewest stations within the same grid.

Analysis of Appendix A reveals that only the $0.25^\circ \times 0.25^\circ$, $0.1^\circ \times 0.1^\circ$, and $0.05^\circ \times 0.05^\circ$ grids contain fewer than three stations per grid. Among these options, the $0.1^\circ \times 0.1^\circ$ resolution is the most common among the products (refer to Table 1). Consequently, this resolution is chosen for resampling the products, ensuring consistency in spatial representation across all datasets.

In the literature, various interpolation methods are available for spatially distributing precipitation data [86,87]. These methods prove invaluable when rainfall estimates from multi-sensor source data, initially on one spatial grid, require transformation to another grid with a different spatial resolution [86]. Among the commonly employed interpolation techniques are bilinear [88,89], first-order conservative [90,91], distance-weighted average [88,92,93], and nearest neighbor [94,95] interpolations. These methods, integrated into the SCRIP toolbox (Spherical Coordinate Remapping and Interpolation Package) [88], are applied in this study. Specifically, the algorithms utilized are Remapbil for bilinear interpolation, Remapcon for first-order conservative interpolation, Remapdis for distance-weighted average interpolation, and Remapnn for nearest neighbor interpolation. These algorithms can be executed using the Climate Data Operators (CDO) software v2.2.1, accessible from the Linux terminal.

In this work, the aforementioned interpolation methods are employed to resample the products to a spatial resolution of $0.1^\circ \times 0.1^\circ$. Consequently, products such as ARC2, RFE, MSWEP, IMERGDE, IMERGDF, and IMERGDL, already possessing this spatial resolution, are not subject to resampling.

2.3.3. Evaluation of Gridded Precipitation Products

In this study, the Kling–Gupta Efficiency (KGE) [96] and Percentage Bias (PBIAS) are utilized as metrics to assess the robustness of the products both before and after resampling (refer to Table 2). The KGE is an enhanced version of the Nash criterion (NSE) [97], which incorporates evaluations of correlation (r), bias (β), and variability (α) [96]. KGE values range from $-\infty$ to 1, where a value of 1 indicates a perfect fit to the in situ data [47,98,99].

Table 2. Statistical evaluation criteria, formulae, ranges, and optimum values.

Criteria	Formulas	Extents	Optimum Values
KGE	$1-\sqrt{(r-1)^2+(\beta-1)^2+(\alpha-1)^2}$	$-\infty$, 1	1 (1)
PBIAS (%)	$\left[\frac{\frac{1}{n}\sum_{i=1}^{n}(P_{Est}-P_{Obs})}{\frac{1}{n}\sum_{i=1}^{n}(P_{Obs})}\right]*100$	$-\infty$, $+\infty$	0 (2)

On the other hand, the PBIAS represents the percentage measure of the average difference between two variables [47]. PBIAS values can range from $-\infty$ to $+\infty$, where positive or negative values indicate overestimation or underestimation of the estimated variable, respectively. Values close to 0 suggest a good performance of the evaluated variable. KGE values of 0.5 and PBIAS values of 0 are commonly employed as reference thresholds to differentiate between the best and worst performances of the evaluated variable [47,100,101]. In this study, these thresholds are defined to facilitate a more comprehensive analysis of the results obtained. The red line depicted on the graphs signifies this threshold for each evaluation criterion.

For this study, the functions of these criteria, developed within the hydroGOF package under R [102], are employed.

The KGE (Kling–Gupta Efficiency) is composed of three variables: r, the correlation coefficient; β, the biases; and α, the variability between the two evaluated variables. The PBIAS (Percentage Bias) is defined as the percentage difference between the estimated precipitation (PEst) and the observed precipitation (PObs).

3. Results

The study presents results based on different time steps, both on a global scale covering all three basins and at the individual hydrosystem level for a more detailed analysis. These include (i) daily, (ii) monthly, and (iii) seasonal performances of gridded precipitation products.

Furthermore, minimal discrepancy is observed among the resampling methods. Consequently, only the outcomes of the bilinear method are presented. Figures containing all the results are presented in Appendix B, Figure A1 for the daily time step, Figure A2 for the monthly time step, and Figure A3 for the seasonal time step.

3.1. Product Performance at Daily Time Intervals

In Figure 3, the comprehensive daily performance of the products before and after spatial resampling is illustrated. Analysis of the KGE values reveals that the gridded precipitation estimates exhibit suboptimal performance on a daily scale. Prior to spatial resampling, only RFE, ARC2, CPC, and MSWEP products demonstrated KGE values exceeding 0.5, while CMORPHCRT exhibited an average KGE of 0.5. Notably, spatial resampling marginally enhanced performance, with CPC, CMORPHCRT, and TAMSAT showing improvements of 3%, 4%, and 2%, respectively.

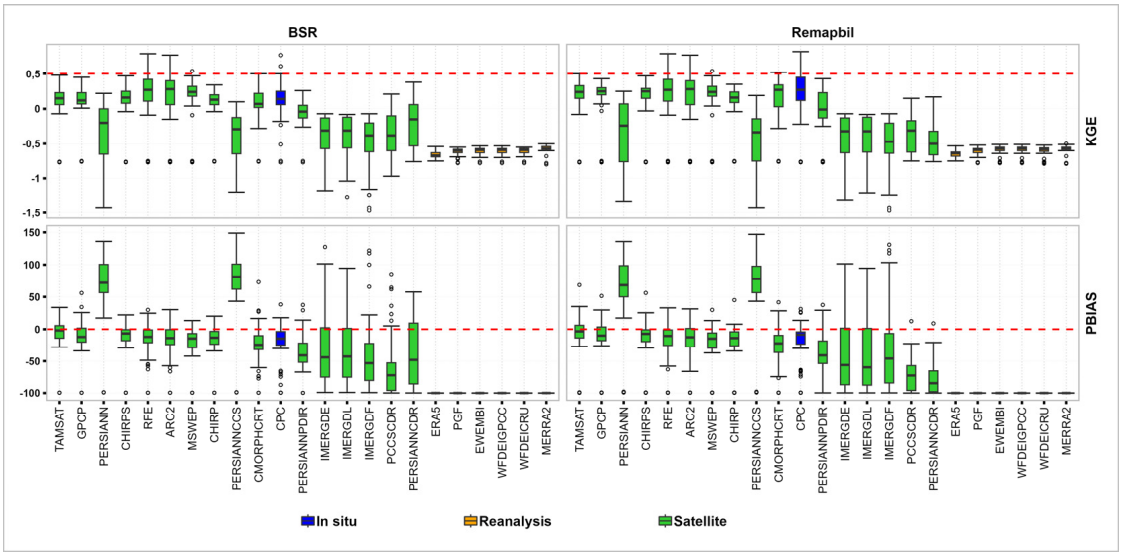

Figure 3. Overall daily performance of products before and after spatial resampling. BSR is "Before Spatial Resampling".

Moreover, all these products exhibited a tendency to slightly underestimate observed rainfall both before and after resampling, as indicated by the PBIAS values. However, products such as IMERGDF, PERSIANNCCS, PERSIANN, IMERGDE, and IMERGDL displayed low KGEs. Notably, PERSIANNCCS and PERSIANN demonstrated substantial overestimations of observed rainfall. Additionally, reanalysis data exhibited limited robustness, consistently providing underestimated values compared to ground data. Among the resampling methods, the nearest neighbor method exhibited the poorest performance.

From a spatial perspective, Figures 4 and 5 depict the spatial distribution of daily KGE values before and after spatial resampling, respectively. It is evident that RFE and ARC2 exhibit reasonable performance in replicating ground rainfall patterns in the Casamance and Senegal basins prior to spatial resampling. However, the performance of these products displays spatial variability within these basins.

In the Casamance basin, RFE and ARC2 demonstrate robustness across all climatic zones, with KGE values ranging from 0.42 to 0.79. Meanwhile, MSWEP exhibits average performance in the Casamance basin. In contrast, in the Senegal River basin, RFE and ARC2 only demonstrate robustness in the Sahelian and Sudanian domains, with KGE values below 0.75.

Furthermore, the performance of CPC notably improves after spatial resampling across all three hydrosystems. Notably, the performance of gridded rainfall products varies across different climatic zones within each basin. Optimal results are observed in the Casamance basin, particularly in the Sudanian zone of the Gambia and the Sahelian and Sudanian domains of the Senegal River basin.

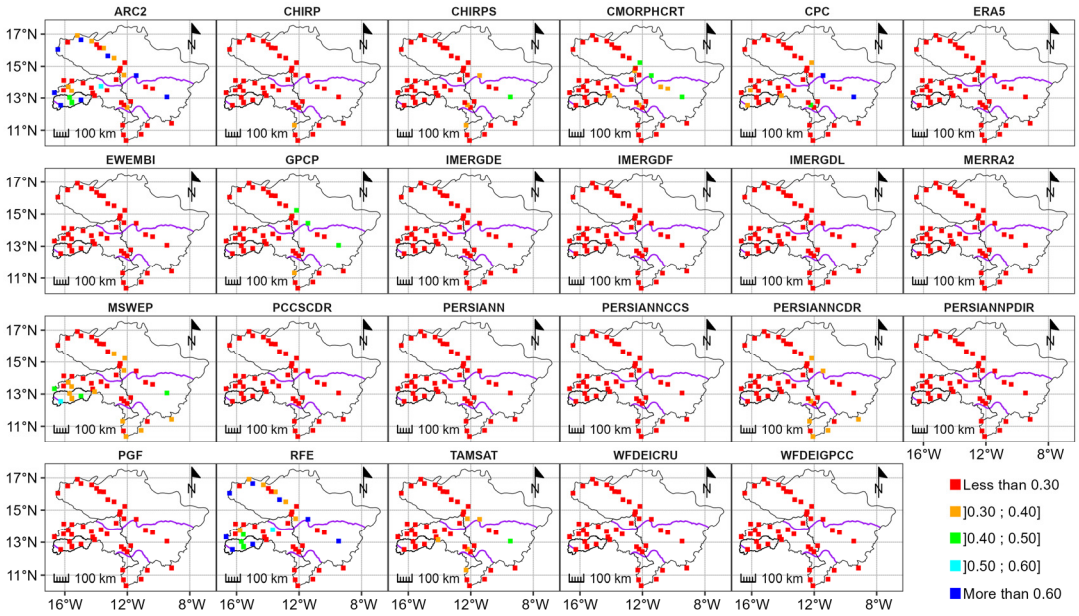

Figure 4. Spatial distribution of daily KGE values for products before spatial resampling.

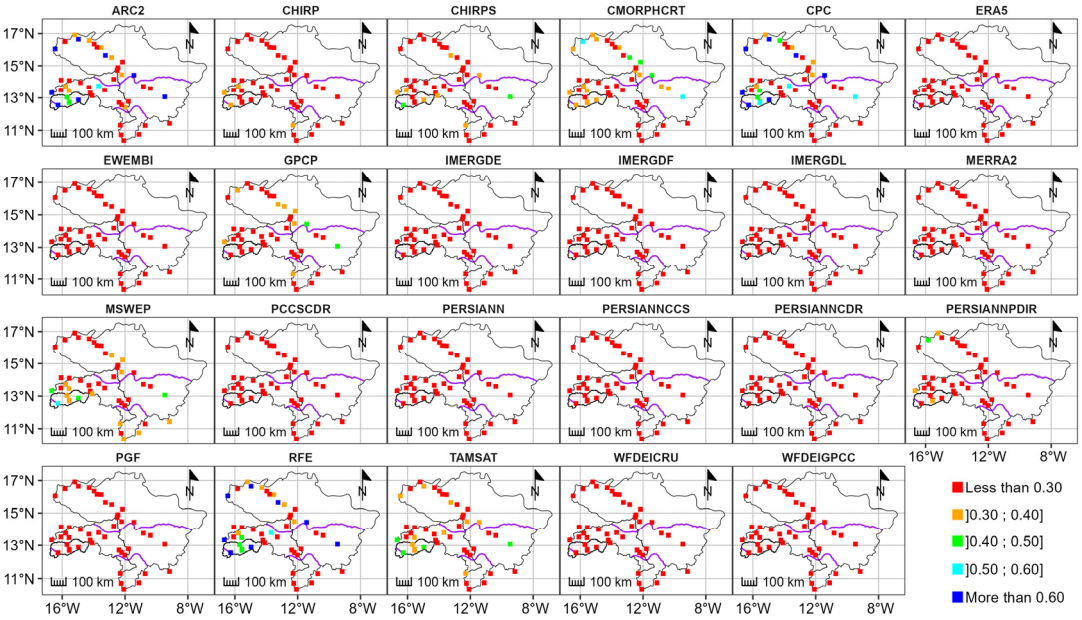

Figure 5. Spatial distribution of daily KGE values for products after spatial resampling using the bilinear method (Remapbil).

3.2. Product Performance at Monthly Intervals

Analysis of the KGE values depicted in Figure 6 reveals that gridded precipitation exhibits greater robustness at the monthly time step compared to the daily time step. Specifically, GPCP, CHIRPS, RFE, MSWEP, ARC2, CPC, CHIRPS, TAMSAT, and CMORPHCRT data demonstrate KGE values ≥ 0.84 at their respective initial resolutions, with relatively low error percentages.

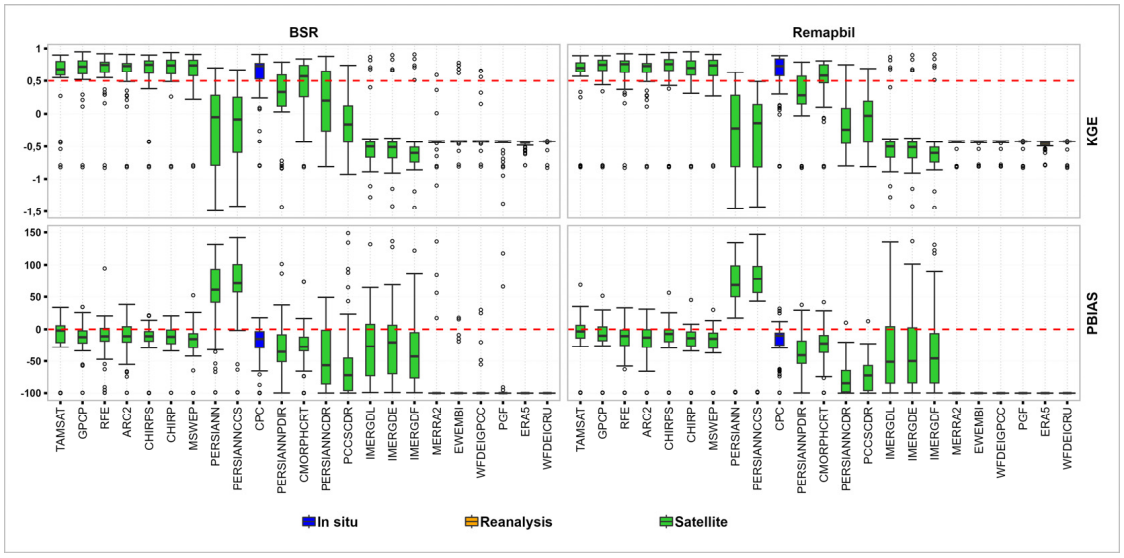

Figure 6. Overall monthly performance of products before and after spatial resampling. BSR is "Before Spatial Resampling".

Spatial resampling resulted in a 4% improvement in KGE values for CHIRPS and a 1% improvement for CHIRP, while CPC, TAMSAT, and CMORPHCRT experienced a 2% deterioration in KGE values. Notably, the GPCP product maintained the same performance as before spatial resampling. However, IMERGDF, PERSIANNCCS, PERSIANN, IMERGDE, and IMERGDL products displayed poor performance at the monthly time step. Analysis of estimation errors indicates that PERSIANNCCS and PERSIANN tend to overestimate observed rainfall. Similar results were observed for the reanalysis products.

Figures 7 and 8 display the spatial distribution of monthly KGE values before and after spatial resampling. These figures illustrate that ARC2, CHIRP, CHIRPS, CMORPHCRT, CPC, GPCP, MSWEP, RFE, and TAMSAT exhibit good agreement with observed data across all climatic domains. However, their performance varies depending on climate zones, basins, and resampling methods.

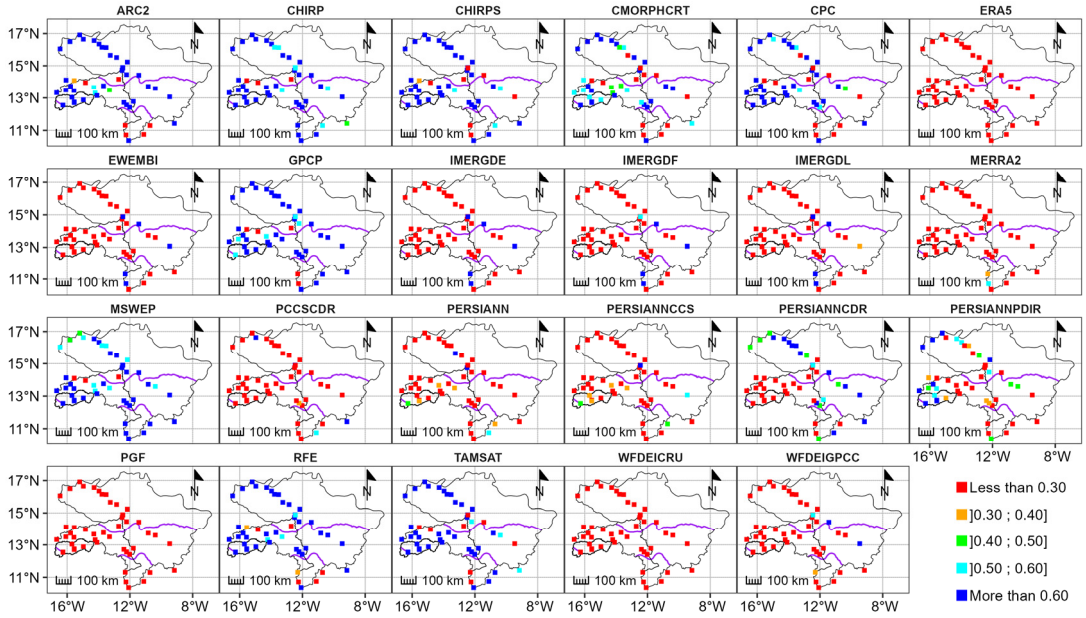

Figure 7. Spatial distribution of monthly KGE values for products before spatial resampling.

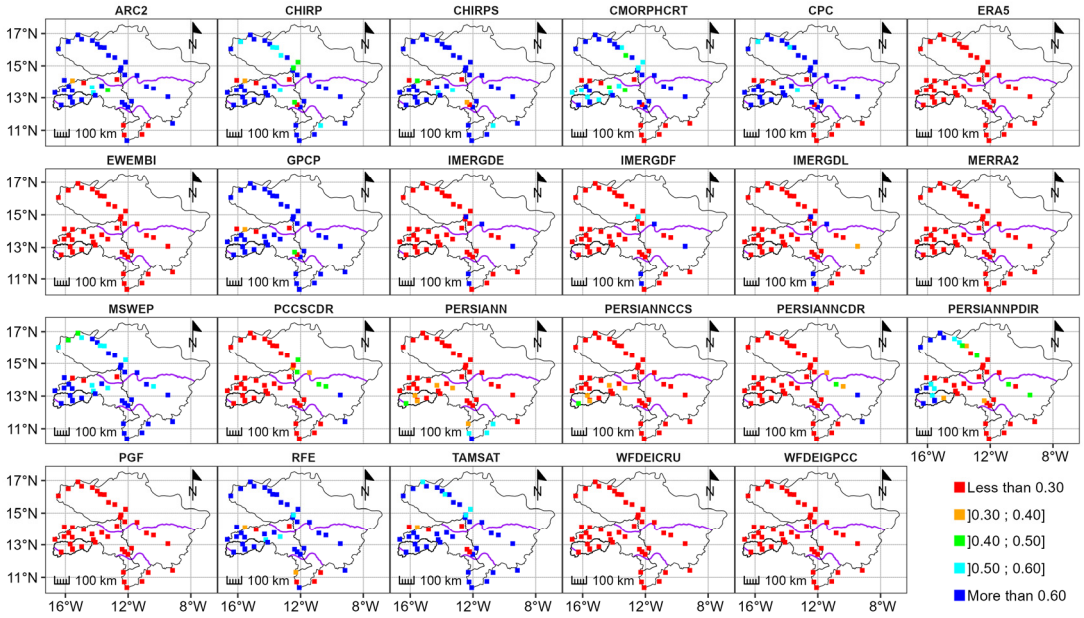

Figure 8. Spatial distribution of monthly KGE values for products after spatial resampling using the bilinear method (Remapbil).

In the Casamance basin, CHIRP, RFE, MSWEP, ARC2, CHIRPS, TAMSAT, CPC, CMORPHCRT, and GPCP products demonstrate robust performance both before and after spatial resampling, with KGE values ranging from 0.33 to 0.94. The most favorable outcomes were observed in the Guinean zone.

Similarly, in the Gambia basin, these products exhibit robustness both before and after spatial resampling, with KGE values fluctuating between −0.8 and 0.94. However, performance varies across different zones, with the Sudanian zone showing the best results.

In the Senegal basin, only CHIRP maintains satisfactory performance both before and after spatial resampling, with KGE values ranging from 0.47 to 0.91. Post-resampling, CHIRPS, GPCP, and TAMSAT exhibit favorable performance across the basin, while CMORPHCRT and CPC show improved performance primarily in the Sahelian and Sudanian climatic zones.

Overall, the most notable performances are observed in the Sahelian and Sudanian climatic zones across all products.

3.3. Seasonal Product Performance

The results regarding the performance of gridded precipitation estimates during the rainy season are depicted in Figure 9. Analysis of this figure reveals that, during the rainy season, the products exhibit performances akin to those obtained at the monthly time step.

Before spatial resampling, RFE, ARC2, MSWEP, CPC, CHIRP, CMORPHCRT, CHIRPS, and GPCP data provide reasonably satisfactory estimates of ground rainfall. Following spatial resampling, the KGE values of GPCP, CHIRPS, CHIRP, and CMORPHCRT improved by 1%, 6%, 9%, 11%, and 19%, respectively, while that of CPC deteriorated by 4%. Additionally, estimation errors for these products decreased.

Conversely, PERSIANN, IMERGDF, EWEMBI, IMERGDE, and IMERGDL yielded the weakest results. PBIAS analysis indicates that PERSIANN and PERSIANNCCS tend to overestimate in situ rainfall during the wet season. Furthermore, during the wet season, the conservative-first and distance-weighted-average methods exhibited the best performance.

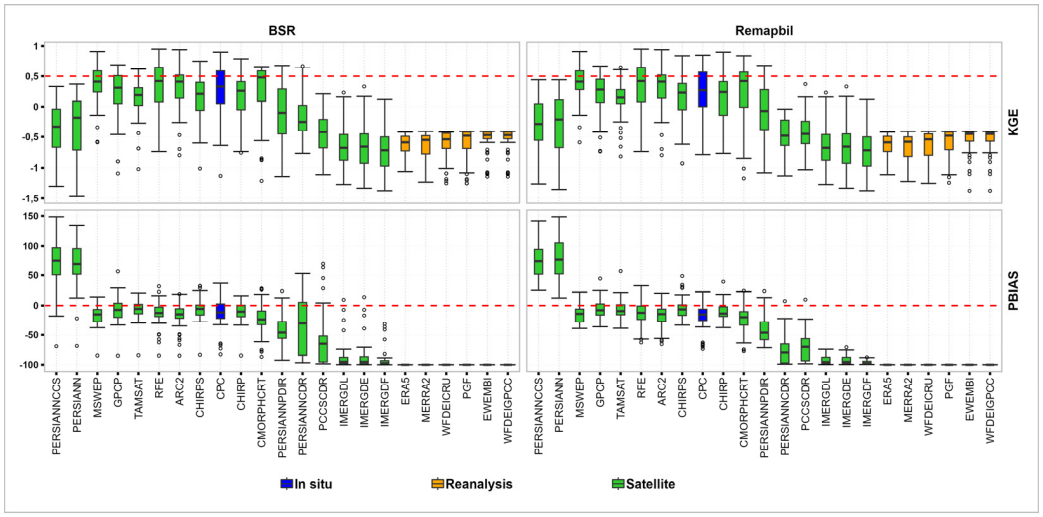

Figure 9. Overall rainy season performance of products before and after spatial resampling. BSR is "Before Spatial Resampling".

Figures 10 and 11 present the spatial distribution of KGE metrics during the rainy season, both pre- and post-spatial resampling. It is evident that the products exhibiting favorable performance during this period correspond to those identified at the monthly temporal scale, namely, ARC2, CHIRP, CHIRPS, CMORPHCRT, CPC, GPCP, MSWEP, and RFE. However, it is noteworthy that the performance of these products varies across different hydrological basins.

In the Casamance basin, ARC2, CHIRP, CHIRPS, CMORPHCRT, CPC, GPCP, MSWEP, and RFE consistently demonstrated robust performance across all climatic zones, with the Guinean zone displaying particularly notable performance. Conversely, within the Gambia basin, these products exhibited divergent performance patterns. Only ARC2 and RFE displayed superior performance across all climatic zones, while CHIRP, CHIRPS, CMORPHCRT, CPC, GPCP, and MSWEP showcased enhanced performance specifically within the Sudanian zone.

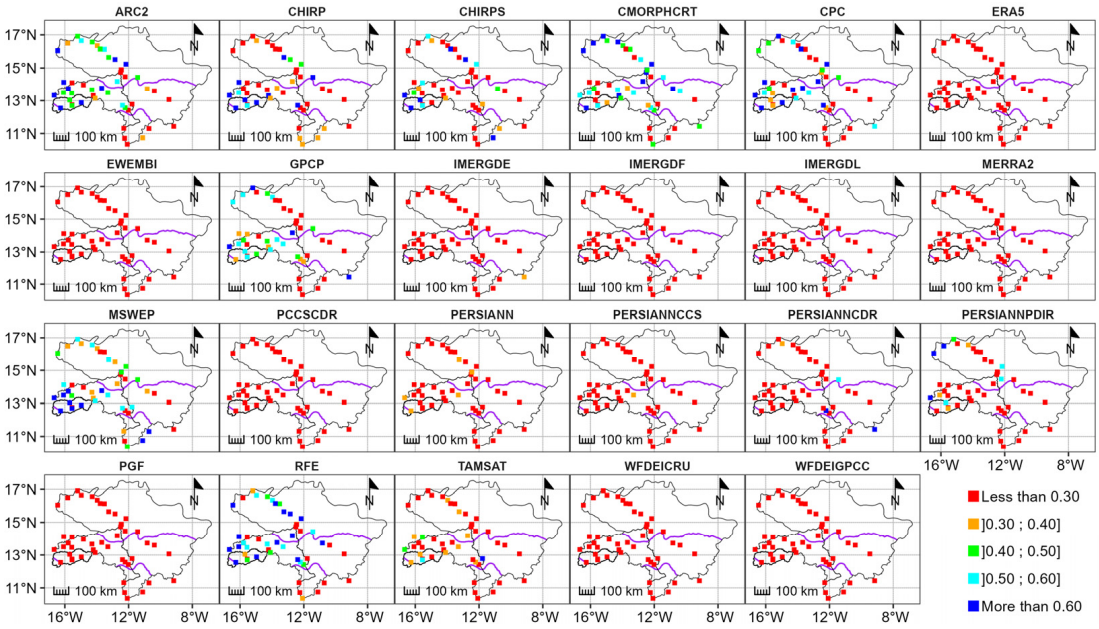

Figure 10. Spatial distribution of rainy season KGE values for products before spatial resampling.

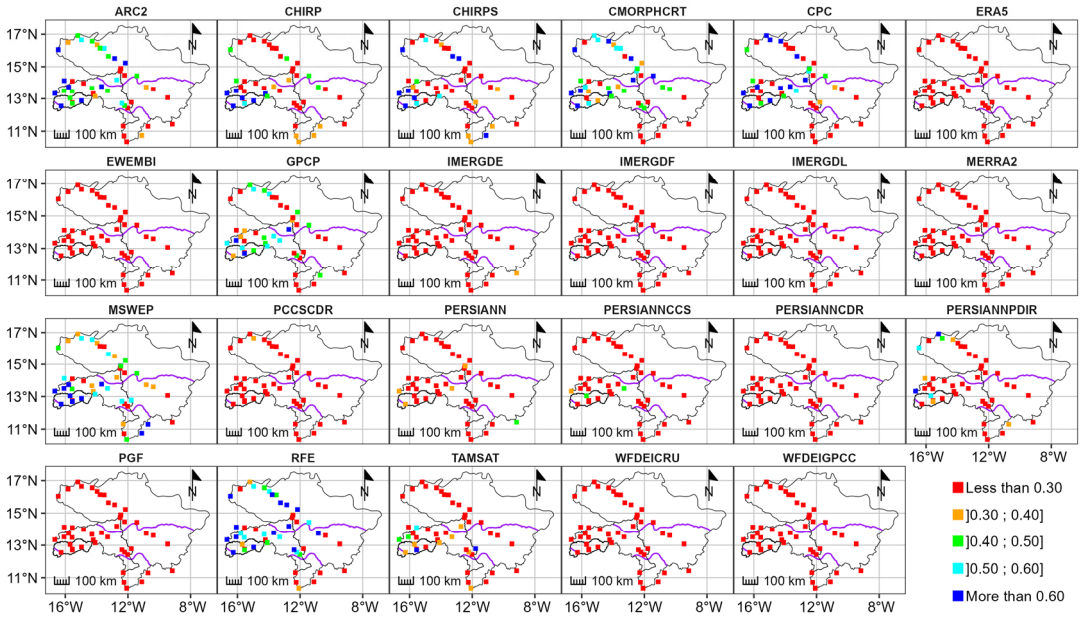

Figure 11. Spatial distribution of rainy season KGE values for products after spatial resampling using the bilinear method (Remapbil).

Within the Senegal basin, ARC2, CMORPHCRT, CPC, and RFE exhibited superior performance in the Sahelian zone. Additionally, MSWEP showcased satisfactory performance throughout the basin, with optimal performance observed within the Guinean zone.

4. Discussion

The analysis of the point-to-pixel comparison between the observed rainfall and gridded rainfall data reveals notable variability in the performance of gridded rainfall datasets contingent upon the temporal resolution and climatic domain. Notably, there is a discernible decrease in performance observed at the daily time step across the board. Beck et al. [60] and Satgé et al. [35] have suggested that such performance discrepancies stem, in part, from discrepancies between the time steps utilized for rain gauge adjustments and the temporal misalignment between rain gauge and satellite reporting times.

ARC2, CPC, and RFE exhibit outstanding performance in rainfall estimation across the Casamance, Gambia, and Senegal basins. Notably, ARC2 and RFE benefit from adjustments based on observed rainfall data, while CPC relies solely on in situ measurements. This differential treatment could elucidate their superior performance. However, the reliability of in situ data also plays a crucial role in shaping the accuracy of corrected gridded rainfall estimates [35]. The absence of reliable in situ measurements hampers local adjustments to satellite-derived estimates, potentially explaining the inefficacy of certain products corrected to the daily time step within the hydrological systems under scrutiny.

The findings resonate with those of Dembélé and Zwart [36] in Burkina Faso, who reported similar outcomes for ARC2 and RFE.

At the monthly temporal scale, a suite of gridded rainfall products including GPCP, CHIRP, CHIRPS, RFE, MSWEP, ARC2, TAMSAT, and CMORPHCRT demonstrate favorable agreement with observed data. Notably, the performance of CHIRPS and MSWEP resonates with findings from Satgé et al. [35] in West Africa, and similarly, Didi et al. [37] underscore the robustness of CHIRPS across five West African nations. This superior performance at monthly scales, compared to daily resolutions, can be attributed to the aggregation effect wherein errors at sub-monthly intervals, partly attributed to temporal misalignment between rain gauge and satellite reporting times, tend to offset one another upon aggregation [36].

At the seasonal scale, particularly during the rainy season, gridded rainfall datasets (RFE, ARC2, MSWEP, CPC, CHIRP, CMORPHCRT, CHIRPS, and GPCP) adequately esti-

mate ground-level precipitation within the studied basins. Nonetheless, it is noted that gridded rainfall estimates are susceptible to seasonal variations, with the consistency of rainfall volumes during winter potentially mitigating errors, while the statistical weight of errors during dry seasons may exacerbate performance discrepancies [35].

From a climatic standpoint, the spatial distribution of Kling–Gupta Efficiency (KGE) values elucidates varying product performances across climatic zones within each basin. Notably, better performances are observed in the Casamance basin overall, the Sudanian zone of the Gambia basin, and the Sahelian and Sudanian climatic zones of the Senegal basin. This disparity in performance can be rationalized by the proximity of these climatic zones to the Atlantic Ocean, facilitating the circulation of colder air masses compared to inland areas. Conversely, the Guinean region in the Gambia and Senegal River basins exhibits poorer performance, attributed to its mountainous terrain and high cloud cover [30,103], which may lead to an overestimation of rainfall due to clouds "not precipitating".

Furthermore, the precipitation bias (PBIAS) analysis indicates that PERSIANN and PERSIANNCCS tend to overestimate observed rainfall, while reanalysis such as ERA5, EWEMBI, MERRA2, PGF, WFDEICRU, and WFDEIGPCC consistently underestimate values. This underestimation or overestimation is often associated with variations in complex topography, with altitude playing a significant role in influencing error magnitude [92].

Regarding spatial resampling, its impact on improving gridded precipitation product results is generally limited, with some data even experiencing performance degradation post-resampling. However, the efficacy of resampling methods varies across products and spatial-temporal scales, with bilinear (Remapbil) exhibiting the most promising results, followed by first-order conservative (Remapcon) and distance-weighted (Remapdis) methods.

The rain gauge stations used in this study are generally located near the main rivers. Thus, there are no stations with data for the period studied in certain parts of the catchment areas used in this work. This situation makes it impossible to obtain an idea of the performance of the data evaluated in these areas. The poor representativeness of the stations used to evaluate gridded rainfall data mainly concerns the Gambia and Senegal River basins. For example, no stations were used in the north-eastern part of the Senegal basin. This limits the robustness of gridded rainfall data in this area.

5. Conclusions

This study endeavors to assess the efficacy of twenty-three gridded rainfall products across West Africa, particularly within the Casamance, Gambia, and Senegal River basins. The methodology encompasses an evaluation of data performance pre- and post-resampling, juxtaposed with observed rainfall data from forty-nine stations over a span of six years (2003–2008) at daily, monthly, and seasonal intervals, utilizing Kling–Gupta Efficiency (KGE) and Percentage Bias (PBIAS) metrics for assessment.

The findings indicate that RFE, ARC2, and CPC demonstrate superior precipitation estimation at the daily time step, while GPCP, CHIRP, CHIRPS, RFE, MSWEP, ARC2, TAMSAT, and CMORPHCRT exhibit greater robustness at monthly intervals. Moreover, RFE, ARC2, MSWEP, CPC, CHIRP, CMORPHCRT, CHIRPS, and GPCP display optimal performance during the rainy season. Spatial analysis of KGE values underscores varying product performance across climatic zones, with the most favorable outcomes observed throughout the Casamance basin and the Sudanian and Sahelian climatic zones of the Gambia and Senegal basins, while subpar performances are typically noted in the Guinean area of the Gambia and Senegal Rivers.

PBIAS results reveal tendencies for PERSIANN and PERSIANNCCS to overestimate precipitation, whereas ERA5, EWEMBI, MERRA2, PGF, WFDEICRU, and WFDEIGPCC consistently underestimate values across spatial and temporal scales. Additionally, resampling efforts exhibit limited efficacy in enhancing product performance, although the Remapbil, Remapcon, and Remapdis methods are recommended for resampling gridded precipitation products within Senegal's primary hydrological systems.

In conclusion, the most efficient products, contingent upon temporal and spatial scales, serve as viable alternatives for diverse hydrological studies in the absence of observed rainfall data within Senegal's main hydrosystems. This study elucidates the strengths and limitations of each product across all examined scales, thereby facilitating informed decision-making for future users. Moreover, the findings provide valuable insights for data-producing organizations and institutions to enhance the accuracy of rainfall estimation algorithms within the study area. However, future endeavors may benefit from hydrological assessments to gauge the products' efficacy in simulating flows.

Author Contributions: Conceptualization, O.G., A.B. and A.D.; methodology, O.G., A.B. and A.D.; software, O.G.; validation, A.B. and A.D.; formal analysis, O.G.; investigation, O.G.; data curation, O.G.; writing—original draft preparation, O.G.; writing—review and editing, O.G, A.B., A.D., I.D. and A.O.; supervision, A.B., A.D. and A.O.; project administration, A.O.; funding acquisition, A.O. All authors have read and agreed to the published version of the manuscript.

Funding: This research was supported by the EU-funded AICS N.03/2020 WEFE-SENEGAL project, the IRD ActNAO International Research Network grants, and the AFD Cycle de l'Eau et Changement Climatique project.

Data Availability Statement: Data will be made available on request.

Acknowledgments: We thank the technical services who provided the observed data and the two reviewers, for their valuable comments which helped strengthen the paper.

Conflicts of Interest: The authors declare no conflicts of interest.

Appendix A. Spatial Resampling of Products

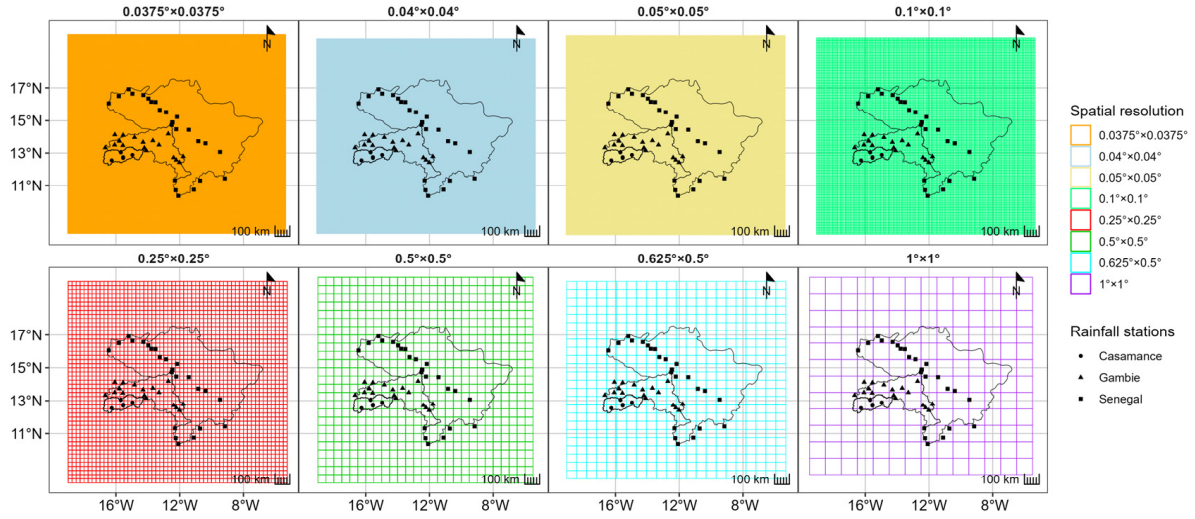

Appendix B. Performance of Products before and after Spatial Resampling

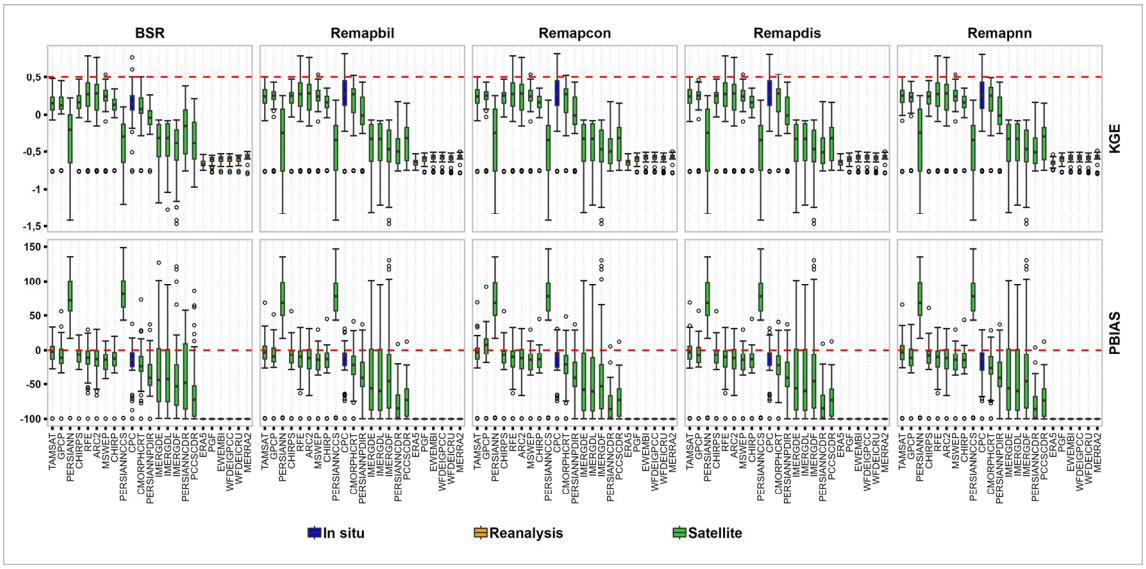

Figure A1. Overall daily performance of products before and after spatial resampling.

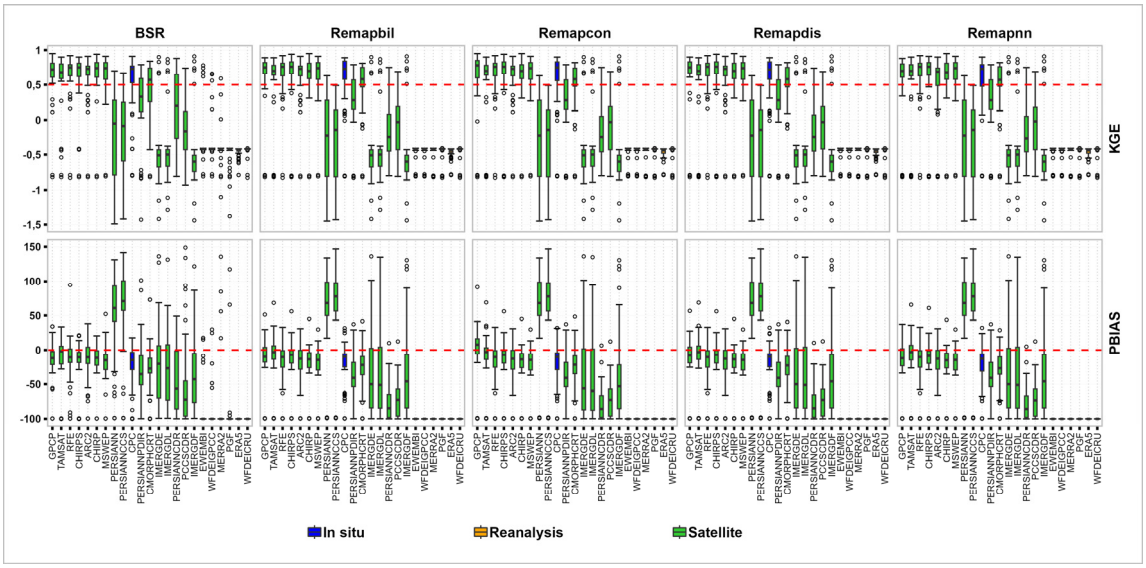

Figure A2. Overall monthly performance of products before and after spatial resampling.

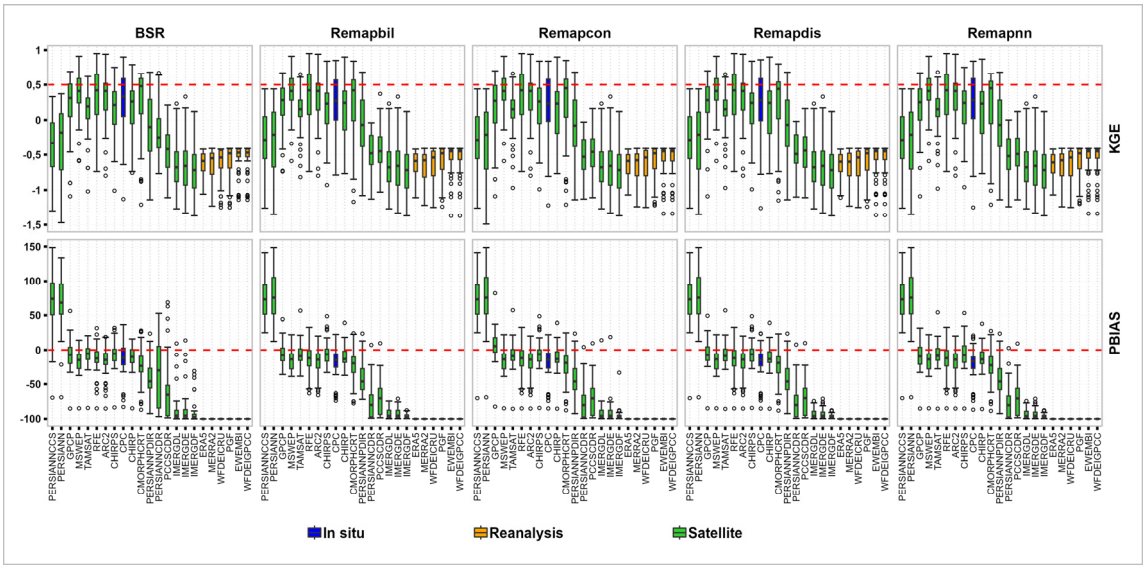

Figure A3. Overall rainy season performance of products before and after spatial resampling.

References

1. Nations, U. *World Population Prospects 2019—Volume II: Demographic Profiles*; Department of Economic and Social Affairs: New York, NY, USA, 2019.
2. Sivakumar, B. Global climate change and its impacts on water resources planning and management: Assessment and challenges. *Stoch. Environ. Res. Risk Assess.* **2011**, *25*, 583–600. [CrossRef]
3. Vargas-Pineda, O.I.; Trujillo-González, J.M.; Torres-Mora, M.A. Supply–demand of water resource of a basin with high anthropic pressure: Case study Quenane-Quenanito Basin in Colombia. *Air Soil Water Res.* **2020**, *13*, 1178622120917725. [CrossRef]
4. Carbonnel, J.P.; Hubert, P. Sur la sécheresse au Sahel d'Afrique de l'Ouest. Une rupture climatique dans les séries pluviométriques du Burkina Faso (ex Haute-Volta). In *Comptes Rendus de l'Académie des Sciences. Série 2, Mécanique, Physique, Chimie, Sciences de l'Univers, Sciences de la Terre*; Bnf Gallica: Paris, France, 1985; Volume 301, pp. 941–944.
5. Nicholson, S.E. The spatial coherence of African rainfall anomalies: Interhemispheric teleconnections. *J. Appl. Meteorol. Climatol.* **1986**, *25*, 1365–1381. [CrossRef]
6. Hubert, P.; Carbonnel, J.P. Approche statistique de l'aridification de l'Afrique de l'Ouest. *J. Hydrol.* **1987**, *95*, 165–183. [CrossRef]
7. Hubert, P.; Carbonnel, J.P.; Chaouche, A. Segmentation des séries hydrométéorologiques—Application à des séries de précipitations et de débits de l'Afrique de l'ouest. *J. Hydrol.* **1989**, *110*, 349–367. [CrossRef]
8. Olivry, J.C.; Bricquet, J.P.; Bamba, F.; Diarra, M. Le régime hydrologique du Niger supérieur et le déficit des deux dernières décennies. In *Quelques Données Préliminaires sur l'Environnement et la Qualité des Apports du Niger au Sahel*; FAO: Washington, DC, USA, 1994; pp. 9–25.
9. Paturel, J.E.; Servat, E.; Kouame, B.; Lubes, H.; Fritsch, J.M.; Masson, J.M. Manifestations d'une variabilité hydrologique en Afrique de l'Ouest et Centrale. *IAHS Publ. Ser. Proc. Rep. Intern. Assoc. Hydrol. Sci.* **1997**, *240*, 21–30.
10. Paturel, J.E.; Servat, E.; Delattre, M.O.; Lubès-Niel, H. Analyse de séries pluviométriques de longue durée en Afrique de l'Ouest et Centrale non sahélienne dans un contexte de variabilité climatique. *Hydrol. Sci. J.* **1998**, *43*, 937–946. [CrossRef]
11. Servat, É.; Paturel, J.E.; Lubès-Niel, H.; Kouamé, B.R.; Masson, J.M.; Travaglio, M.; Marieu, B. De différents aspects de la variabilité de la pluviométrie en Afrique de l'Ouest et Centrale non sahélienne. *Rev. Sci. L'Eau* **1999**, *12*, 363–387. [CrossRef]
12. Nicholson, S.E.; Some, B.; Kone, B. An analysis of recent rainfall conditions in West Africa, including the rainy seasons of the 1997 El Niño and the 1998 La Niña years. *J. Clim.* **2000**, *13*, 2628–2640. [CrossRef]
13. Dacosta, H.; Kandia, K.Y.; Malou, R. *La Variabilité Spatio-Temporelle des Précipitations au Sénégal depuis un Siècle*; IAHS Press: Wallingford, UK, 2002; pp. 499–506.
14. Mahé, G.; Paturel, J.E. 1896–2006 Sahelian annual rainfall variability and runoff increase of Sahelian Rivers. *Comptes Rendus Geosci.* **2009**, *341*, 538–546. [CrossRef]
15. Bodian, A.; Dacosta, H.; Dezetter, A. Caractérisation spatio-temporelle du régime pluviométrique du haut bassin du fleuve Sénégal dans un contexte de variabilité climatique. *Physio-Géo. Géographie Phys. Environ.* **2011**, *5*, 107–124. [CrossRef]
16. Descroix, L.; Djiba, S.; Sané, T.; Tarchiani, V. *Eaux et Sociétés Face au Changement Climatique dans le Bassin de la Casamance: Actes de l'Atelier Scientifique et du Lancement de l'Initiative "Casamance: Un Réseau Scientifique au Service du Développement en Casamance" du 15–17 Juin 2015 à Hôtel KADIANDOUMAGNE de Ziguinchor, Sénégal*; HAL Open Science: Lyon, France, 2015.
17. Gascon, T. Impact de la Résolution Spatiale et Temporelle des Entrées Pluviométriques pour la Modélisation Hydrologique en Afrique de l'Ouest et Implication dans l'utilisation des Produits Satellitaires: Etude de Cas sur le Bassin de l'Ouémé au Benin. Ph.D. Thesis, Université Grenoble Alpes, Grenoble, France, 2016; 240p.

18. Deme, A.; Gaye, A.T.; Hourdin, F. Les projections du climat. In *Les Sociétés Rurales Face aux Changements Climatiques et Environnementaux en Afrique de l'Ouest*; IRD Editions: Paris, France, 2017; p. 61.
19. Baron, C.; Bonnassieux, A. Les enjeux de l'accès à l'eau en Afrique de l'Ouest: Diversité des modes de gouvernance et conflits d'usages. *Monde Dév.* **2011**, *4*, 17–32. [CrossRef]
20. Biswas, A.K. Integrated water resources management: A reassessment: A water forum contribution. *Water Int.* **2004**, *29*, 248–256. [CrossRef]
21. Savenije, H.H.; Van der Zaag, P. Integrated water resources management: Concepts and issues. *Phys. Chem. Earth Parts A/B/C* **2008**, *33*, 290–297. [CrossRef]
22. El Bedawy, R. Water resources management: Alarming crisis for Egypt. *J. Mgmt. Sustain.* **2014**, *4*, 108. [CrossRef]
23. Dörfliger, N.; Perrin, J. Ressources en eau: Une gestion nécessairement locale dans une approche globale. *Geosciences* **2011**, *13*, 94–101.
24. Bodian, A.; Dezetter, A.; Dacosta, H. Apport de la modélisation pluie-débit pour la connaissance de la ressource en eau: Application au haut bassin du fleuve Sénégal. *Climatologie* **2012**, *9*, 109–125. [CrossRef]
25. Faye, C. Gestion des Ressources en Eau en Afrique: Problèmes de Disponibilité des Données et Incertitudes Associées aux Mesures Hydrologiques au Sénégal. In Proceedings of the Congrès SHF: Hydrométrie 2017, Lyon, France, 14–15 March 2017.
26. Bodian, A.; Diop, L.; Panthou, G.; Dacosta, H.; Deme, A.; Dezetter, A.; Ndiaye, P.M.; Diouf, I.; Vichel, T. Recent trend in hydroclimatic conditions in the Senegal River Basin. *Water* **2020**, *12*, 436. [CrossRef]
27. Nicholson, S.E.; Some, B.; McCollum, J.; Nelkin, E.; Klotter, D.; Berte, Y.; Traore, A.K. Validation of TRMM and other rainfall estimates with a high-density gauge dataset for West Africa. Part II: Validation of TRMM rainfall products. *J. Appl. Meteorol.* **2003**, *42*, 1355–1368. [CrossRef]
28. Bodian, A. Caractérisation de la variabilité temporelle récente des précipitations annuelles au Sénégal (Afrique de l'Ouest). *Physio-Géo. Géographie Phys. Environ.* **2014**, *8*, 297–312. [CrossRef]
29. Tramblay, Y.; El Khalki, E.M.; Ciabatta, L.; Camici, S.; Hanich, L.; Saidi, M.E.M.; Brocca, L. River runoff estimation with satellite rainfall in Morocco. *Hydrol. Sci. J.* **2023**, *68*, 474–487. [CrossRef]
30. Arkin, P.A.; Ardanuy, P.E. Estimating climatic-scale precipitation from space: A review. *J. Clim.* **1989**, *2*, 1229–1238. [CrossRef]
31. Ashouri, H.; Hsu, K.L.; Sorooshian, S.; Braithwaite, D.K.; Knapp, K.R.; Cecil, L.D.; Prat, O.P. PERSIANN-CDR: Daily precipitation climate data record from multisatellite observations for hydrological and climate studies. *Bull. Am. Meteorol. Soc.* **2015**, *96*, 69–83. [CrossRef]
32. Jiang, S.; Zhang, Z.; Huang, Y.; Chen, X.; Chen, S. Evaluating the TRMM multisatellite precipitation analysis for extreme precipitation and streamflow in Ganjiang River basin, China. *Adv. Meteorol.* **2017**, *2017*, 2902493. [CrossRef]
33. Centella-Artola, A.; Bezanilla-Morlot, A.; Taylor, M.A.; Herrera, D.A.; Martinez-Castro, D.; Gouirand, I.; Alpizar, M. Evaluation of sixteen gridded precipitation datasets over the Caribbean region using gauge observations. *Atmosphere* **2020**, *11*, 1334. [CrossRef]
34. Thiemig, V.; Rojas, R.; Zambrano-Bigiarini, M.; De Roo, A. Hydrological evaluation of satellite-based rainfall estimates over the Volta and Baro-Akobo Basin. *J. Hydrol.* **2013**, *499*, 324–338. [CrossRef]
35. Satgé, F.; Defrance, D.; Sultan, B.; Bonnet, M.-P.; Seyler, F.; Rouché, N.; Pierron, F.; Paturel, J.-E. Evaluation of 23 gridded precipitation datasets across West Africa. *J. Hydrol.* **2020**, *581*, 124412. [CrossRef]
36. Dembélé, M.; Zwart, S.J. Evaluation and comparison of satellite-based rainfall products in Burkina Faso, West Africa. *Int. J. Remote Sens.* **2016**, *37*, 3995–4014. [CrossRef]
37. Didi, S.R.M.; Ly, M.; Kouakou, K.; Adeline, B.; Diédhiou, A.; Coulibaly, H.S.J.; Kaoudio, K.C.A.; Coulibaly, T.J.H.; Obahoundje Issiaka, S. Using the CHIRPS dataset to investigate historical changes in precipitation extremes in West Africa. *Climate* **2020**, *8*, 84. [CrossRef]
38. Stisen, S.; Sandholt, I. Evaluation of remote-sensing-based rainfall products through predictive capability in hydrological runoff modelling. *Hydrol. Process. Int. J.* **2010**, *24*, 879–891. [CrossRef]
39. Gosset, M.; Viarre, J.; Quantin, G.; Alcoba, M. Evaluation of several rainfall products used for hydrological applications over West Africa using two high-resolution gauge networks. *Q. J. R. Meteorol. Soc.* **2013**, *139*, 923–940. [CrossRef]
40. Casse, C.; Gosset, M.; Peugeot, C.; Pedinotti, V.; Boone, A.; Tanimoun, B.A.; Decharme, B. Potential of satellite rainfall products to predict Niger River flood events in Niamey. *Atmos. Res.* **2015**, *163*, 162–176. [CrossRef]
41. Bodian, A.; Dezetter, A.; Deme, A.; Diop, L. Hydrological evaluation of TRMM rainfall over the upper Senegal River basin. *Hydrology* **2016**, *3*, 15. [CrossRef]
42. Poméon, T.; Jackisch, D.; Diekkrüger, B. Evaluating the performance of remotely sensed and reanalysed precipitation data over West Africa using HBV light. *J. Hydrol.* **2017**, *547*, 222–235. [CrossRef]
43. Bâ, K.M.; Balcázar, L.; Diaz, V.; Ortiz, F.; Gómez-Albores, M.A.; Díaz-Delgado, C. Hydrological evaluation of PERSIANN-CDR rainfall over Upper Senegal River and Bani River basins. *Remote Sens.* **2018**, *10*, 1884. [CrossRef]
44. Dembélé, M.; Schaefli, B.; van de Giesen, N.; Mariéthoz, G. Suitability of 17 rainfall and temperature gridded datasets for largescale hydrological modelling in West Africa. *Hydrol. Earth Syst. Sci. Discuss.* **2020**, *2020*, 1–39.
45. Kouakou, C.; Paturel, J.E.; Satgé, F.; Tramblay, Y.; Defrance, D.; Rouché, N. Comparison of gridded precipitation estimates for regional hydrological modeling in West and Central Africa. *J. Hydrol. Reg. Stud.* **2023**, *47*, 101409. [CrossRef]

46. Faye, C. méthode d'analyse statistique de données morphométriques: Corrélation de paramètres morphométriques et influence sur l'écoulement des sous-bassins du fleuve Sénégal. *Cinq Cont.* **2014**, *4*, 80–108.
47. Ndiaye, M.P. Evaluation, Calibration et Analyse des Tendances Actuelles et Futures de l'Évapotranspiration de Référence dans le Bassin du Fleuve Sénégal. Ph.D. Thesis, Université Gaston Berger, Saint-Louis, Senegal, 2021; 169p.
48. OMVS; HAUT-COMMISSARIAT. Projet de gestion des ressources en eau et de l'environnement du bassin du fleuve Sénégal: Composante 3: Analyse Diagnostique Transfrontalière et Plan d'Action Stratégique. In *OMVS, Analyse Diagnostique Environnementale Transfrontalière du Bassin du Fleuve Sénégal, Synthèse Régionale*; Rapport Final; African Water Information System: Dakar, Sénégal, 2007; 139p.
49. Lamagat, J.P. *Monographie Hydrologique du Fleuve Gambie Collection M&m*; ORSTOM-OMVG: Dakar, Senegal, 1989; 250p.
50. Faye, C. Caractérisation d'un bassin versant par l'analyse statistique des paramètres morphométriques: Cas du bassin versant de la Gambie (bassin continental Guineo-Sénégalais). *Rev. Marocaine Géomorphologie* **2018**, *2*, 110–127.
51. Lamagat, J.P.; Albergel, J.; Bouchez, J.M.; Descroix, L. Monographie hydrologique du fleuve Gambie. In *Ouvrage Publié avec le Concours du Ministère Français de la Cooperation*; HAL Open Science: Lyon, France, 1990; 256p.
52. Dacosta, H. Précipitations et Écoulements sur le Bassin de la Casamance. Ph.D. Thesis, Université Cheikh Anta Diop, Dakar, Senegal, 1989.
53. Bodian, A.; Bacci, M.; Diop, M. *Impact potentiel du changement climatique sur les ressources en eau de surface du bassin de la Casamance à partir des scénarios du CMIP5*; Rapport n. 16; Programme d'Appui au Programme National d'Investissement en Agriculture du Sénégal (PAPSEN): Sédhiou, Sénégal, 2015; pp. 13–16+49.
54. Sadio, P.M.; Mbaye, M.L.; Diatta, S.; Sylla, M.B. Hydro-climate variability and change in the Casamance river basin (Senegal). *Houille Blanche-Rev. Int. L'Eau* **2021**, *6*, 89–96.
55. Vintrou, E. Cartographie et Caractérisation des Systèmes Agricoles au Mali par Télédétection à Moyenne Résolution Spatiale. Ph.D. Thesis, AgroParisTech, Paris, France, 2012.
56. Novella, N.S.; Thiaw, W.M. African rainfall climatology version 2 for famine early warning systems. *J. Appl. Meteorol. Climatol.* **2013**, *52*, 588–606. [CrossRef]
57. Funk, C.; Peterson, P.; Landsfeld, M.; Pedreros, D.; Verdin, J.; Shukla, S.; Michaelsen, J. The climate hazards infrared precipitation with stations—A new environmental record for monitoring extremes. *Sci. Data* **2015**, *2*, 1–21. [CrossRef] [PubMed]
58. Beck, H.E.; Van Dijk, A.I.; Levizzani, V.; Schellekens, J.; Miralles, D.G.; Martens, B.; Roo, A.D. MSWEP: 3-hourly 0.25 global gridded precipitation (1979–2015) by merging gauge, satellite, and reanalysis data. *Hydrol. Earth Syst. Sci.* **2017**, *21*, 589–615. [CrossRef]
59. Beck, H.E.; Wood, E.F.; Pan, M.; Fisher, C.K.; Miralles, D.G.; van Dijk, A.I.J.M.; Adler, R.F. MSWEP V2 global 3-hourly 0.1 precipitation: Methodology and quantitative assessment. *Bull. Am. Meteorol. Soc.* **2019**, *100*, 473–500. [CrossRef]
60. Beck, H.E.; Pan, M.; Roy, T.; Weedon, G.P.; Pappenberger, F.; Van Dijk, A.I.; Wood, E.F. Daily evaluation of 26 precipitation datasets using Stage-IV gauge-radar data for the CONUS. *Hydrol. Earth Syst. Sci.* **2019**, *23*, 207–224. [CrossRef]
61. Tarnavsky, E.; Grimes, D.; Maidment, R.; Black, E.; Allan, R.P.; Stringer, M.; Kayitakire, F. Extension of the TAMSAT satellite-based rainfall monitoring over Africa and from 1983 to present. *J. Appl. Meteorol. Climatol.* **2014**, *53*, 2805–2822. [CrossRef]
62. Maidment, R.I.; Grimes, D.; Black, E.; Tarnavsky, E.; Young, M.; Greatrex, H.; Alcántara, E.M.U. A new, long-term daily satellite-based rainfall dataset for operational monitoring in Africa. *Sci. Data* **2017**, *4*, 170063. [CrossRef] [PubMed]
63. Huffman, G.J.; Adler, R.F.; Morrissey, M.M.; Bolvin, D.T.; Curtis, S.; Joyce, R.; Susskind, J. Global precipitation at one-degree daily resolution from multisatellite observations. *J. Hydrometeorol.* **2001**, *2*, 36–50. [CrossRef]
64. Hsu, K.L.; Gao, X.; Sorooshian, S.; Gupta, H.V. Precipitation estimation from remotely sensed information using artificial neural networks. *J. Appl. Meteorol. Climatol.* **1997**, *36*, 1176–1190. [CrossRef]
65. Sorooshian, S.; Hsu, K.L.; Gao, X.; Gupta, H.V.; Imam, B.; Braithwaite, D. Evaluation of PERSIANN system satellite-based estimates of tropical rainfall. *Bull. Am. Meteorol. Soc.* **2000**, *81*, 2035–2046. [CrossRef]
66. Hong, Y.; Hsu, K.L.; Sorooshian, S.; Gao, X. Precipitation estimation from remotely sensed imagery using an artificial neural network cloud classification system. *J. Appl. Meteorol.* **2004**, *43*, 1834–1853. [CrossRef]
67. Nguyen, P.; Ombadi, M.; Gorooh, V.A.; Shearer, E.J.; Sadeghi, M.; Sorooshian, S.; Ralph, M.F. Persiann dynamic infrared–rain rate (PDIR-now): A near-real-time, quasi-global satellite precipitation dataset. *J. Hydrometeorol.* **2020**, *21*, 2893–2906. [CrossRef]
68. Sadeghi, M.; Nguyen, P.; Naeini, M.R.; Hsu, K.; Braithwaite, D.; Sorooshian, S. PERSIANN-CCS-CDR, a 3-hourly 0.04 global precipitation climate data record for heavy precipitation studies. *Sci. Data* **2021**, *8*, 157. [CrossRef]
69. Joyce, R.J.; Janowiak, J.E.; Arkin, P.A.; Xie, P. CMORPH: A method that produces global precipitation estimates from passive microwave and infrared data at high spatial and temporal resolution. *J. Hydrometeorol.* **2004**, *5*, 487–503. [CrossRef]
70. Xie, P.; Joyce, R.; Wu, S.; Yoo, S.H.; Yarosh, Y.; Sun, F.; Lin, R. Reprocessed, bias-corrected CMORPH global high-resolution precipitation estimates from 1998. *J. Hydrometeorol.* **2017**, *18*, 1617–1641. [CrossRef]
71. Xie, P.; Arkin, P.A. Analyses of global monthly precipitation using gauge observations, satellite estimates, and numerical model predictions. *J. Clim.* **1996**, *9*, 840–858. [CrossRef]
72. Herman, A.; Kumar, V.B.; Arkin, P.A.; Kousky, J.V. Objectively determined 10-day African rainfall estimates created for famine early warning systems. *Int. J. Remote Sens.* **1997**, *18*, 2147–2159. [CrossRef]

73. Huffman, G.J.; Bolvin, D.T.; Braithwaite, D.; Hsu, K.L.; Joyce, R.J.; Kidd, C.; Xie, P. Integrated multi-satellite retrievals for the global precipitation measurement (GPM) mission (IMERG). *Satell. Precip. Meas.* **2020**, *1*, 343–353.
74. Gelaro, R.; McCarty, W.; Suárez, M.J.; Todling, R.; Molod, A.; Takacs, L.; Zhao, B. The modern-era retrospective analysis for research and applications, version 2 (MERRA-2). *J. Clim.* **2017**, *30*, 5419–5454. [CrossRef] [PubMed]
75. Reichle, R.H.; Draper, C.S.; Liu, Q.; Girotto, M.; Mahanama, S.P.P.; Koster, R.D.; De Lannoy, G.J.M. Assessment of MERRA-2 land surface hydrology estimates. *J. Clim.* **2017**, *30*, 2937–2960. [CrossRef]
76. Hersbach, H.; de Rosnay, P.; Bell, B.; Schepers, D.; Simmons, A.; Soci, C.; Abdalla, S.; Alonso-Balmaseda, M.; Balsamo, G.; Bechtold, P.; et al. *Operational Global Reanalysis: Progress, Future Directions and Synergies with NWP*; ERA Report Series; ECMWF: Reading, UK, 2018.
77. Lange, S. *EartH2Observe, WFDEI and ERA-Interim Data Merged and Bias-Corrected for ISIMIP (EWEMBI)*; GFZ Data Services; PIK: Potsdam, Germany, 2016.
78. Sheffield, J.; Goteti, G.; Wood, E.F. Development of a 50-year high-resolution global dataset of meteorological forcings for land surface modeling. *J. Clim.* **2006**, *19*, 3088–3111. [CrossRef]
79. Weedon, G.P.; Balsamo, G.; Bellouin, N.; Gomes, S.; Best, M.J.; Viterbo, P. The WFDEI meteorological forcing data set: WATCH Forcing Data methodology applied to ERA-Interim reanalysis data. *Water Resour. Res.* **2014**, *50*, 7505–7514. [CrossRef]
80. Xie, P.; Chen, M.; Yang, S.; Yatagai, A.; Hayasaka, T.; Fukushima, Y.; Liu, C. A gauge-based analysis of daily precipitation over East Asia. *J. Hydrometeorol.* **2007**, *8*, 607–626. [CrossRef]
81. Chen, M.; Shi, W.; Xie, P.; Silva, V.B.; Kousky, V.E.; Wayne Higgins, R.; Janowiak, J.E. Assessing objective techniques for gauge-based analyses of global daily precipitation. *J. Geophys. Res. Atmos.* **2008**, *113*, D4. [CrossRef]
82. Levizzani, V.; Bauer, P.; Turk, F.J. *Measuring Precipitation from Space: EURAINSAT and the Future*; Springer Science & Business Media: Berlin/Heidelberg, Germany, 2007; Volume 28.
83. Nguyen, P.; Ombadi, M.; Sorooshian, S.; Hsu, K.; AghaKouchak, A.; Braithwaite, D.; Thorstensen, A.R. The PERSIANN family of global satellite precipitation data: A review and evaluation of products. *Hydrol. Earth Syst. Sci.* **2018**, *22*, 5801–5816. [CrossRef]
84. Levizzani, V.; Kidd, C.; Kirschbaum, D.B.; Kummerow, C.D.; Nakamura, K.; Turk, F.J. *Satellite Precipitation Measurement*; Springer: Cham, Switzerland, 2020.
85. Balme, M.; Galle, S.; Lebel, T. Démarrage de la saison des pluies au Sahel: Variabilité aux échelles hydrologique et agronomique, analysée à partir des données EPSAT-Niger. *Sécheresse* **2005**, *16*, 15–22.
86. Teegavarapu, R.S.; Meskele, T.; Pathak, C.S. Geo-spatial grid-based transformations of precipitation estimates using spatial interpolation methods. *Comput. Geosci.* **2012**, *40*, 28–39. [CrossRef]
87. Da Silva, A.S.A.; Stosic, B.; Menezes, R.S.C.; Singh, V.P. Comparison of interpolation methods for spatial distribution of monthly precipitation in the state of Pernambuco, Brazil. *J. Hydrol. Eng.* **2019**, *24*, 04018068. [CrossRef]
88. Jones, P.W. *A User's Guide for SCRIP: A Spherical Coordinate Remapping and Interpolation Package*; Los Alamos National Laboratory: Los Alamos, NM, USA, 1998.
89. Kim, K.H.; Shim, P.S.; Shin, S. An alternative bilinear interpolation method between spherical grids. *Atmosphere* **2019**, *10*, 123. [CrossRef]
90. Jones, P.W. First-and second-order conservative remapping schemes for grids in spherical coordinates. *Mon. Weather Rev.* **1999**, *127*, 2204–2210. [CrossRef]
91. Diaconescu, E.P.; Gachon, P.; Laprise, R. On the remapping procedure of daily precipitation statistics and indices used in regional climate model evaluation. *J. Hydrometeorol.* **2015**, *16*, 2301–2310. [CrossRef]
92. Tomczak, M. Spatial interpolation and its uncertainty using automated anisotropic inverse distance weighting (IDW)-cross-validation/jackknife approach. *J. Geogr. Inf. Decis. Anal.* **1998**, *2*, 18–30.
93. Olaofe, Z.O. On the remapping and identification of potential wind sites in nigeria. *Energy Power Eng.* **2015**, *7*, 477–499. [CrossRef]
94. Jorgensen, D.P.; Hildebrand, P.H.; Frush, C.L. Feasibility test of an airborne pulse—Doppler meteorological radar. *J. Appl. Meteorol. Climatol.* **1983**, *22*, 744–757. [CrossRef]
95. Sharif, H.O.; Ogden, F.L. Mass-conserving remapping of radar data onto two-dimensional cartesian coordinates for hydrologic applications. *J. Hydrometeorol.* **2014**, *15*, 2190–2202. [CrossRef]
96. Gupta, H.V.; Kling, H.; Yilmaz, K.K.; Martinez, G.F. Decomposition of the mean squared error and NSE performance criteria: Implications for improving hydrological modelling. *J. Hydrol.* **2009**, *377*, 80–91. [CrossRef]
97. Nash, J.E.; Sutcliffe, J.V. River flow forecasting through conceptual models part I—A discussion of principles. *J. Hydrol.* **1970**, *10*, 282–290. [CrossRef]
98. Knoben, W.J.; Freer, J.E.; Woods, R.A. Inherent benchmark or not? Comparing Nash–Sutcliffe and Kling–Gupta efficiency scores. *Hydrol. Earth Syst. Sci.* **2019**, *23*, 4323–4331. [CrossRef]
99. Vrugt, J.A.; de Oliveira, D.Y. Confidence intervals of the Kling-Gupta efficiency. *J. Hydrol.* **2022**, *612*, 127968. [CrossRef]
100. Diop, S.B. Evaluation, Calibration et Analyse des Tendances de l'Évapotranspiration de Référence dans les Bassins des Fleuves Casamance et Gambie. Master's Thesis, Université Gaston Berger, Saint-Louis, Senegal, 2021; 68p.
101. Gaye, I.T. Modélisation des Impacts du Changement Climatique sur les Ressources en Eau du Bassin Versant du Bafing (Haut Bassin du Fleuve du Sénégal). Master's Thesis, Université Assane Seck de Ziguinchor, Ziguinchor, Senegal, 2022; 69p.

102. Zambrano-Bigiarini, M. *Package 'hydroGOF'. Goodness-of-Fit Functions for Comparison of Simulated and Observed*, Version 0.6-0; R Core Team: Vienna, Austria, 2017.
103. Sharifi, E.; Saghafian, B.; Steinacker, R. Downscaling satellite precipitation estimates with multiple linear regression, artificial neural networks, and spline interpolation techniques. *J. Geophys. Res. Atmos.* **2019**, *124*, 789–805. [CrossRef]